Interactions between Ground State Oxygen Atoms and Molecules: O—O and O_2—O_2

JOSEPH T. VANDERSLICE, EDWARD A. MASON, AND WILLIAM G. MAISCH

Reprinted from THE JOURNAL OF CHEMICAL PHYSICS, Vol. 32, No. 2, pp. 515–524, February, 1960

Reprinted from the JOURNAL OF CHEMICAL PHYSICS, Vol. 32, No. 2, 515–524, February, 1960
Printed in U. S. A.

Interactions between Ground State Oxygen Atoms and Molecules: O—O and O_2—O_2*

JOSEPH T. VANDERSLICE, EDWARD A. MASON, AND WILLIAM G. MAISCH
Institute for Molecular Physics, University of Maryland, College Park, Maryland

(Received June 22, 1959)

Potential energy curves for O—O interactions corresponding to the $X\,^3\Sigma_g^-$, $^1\Delta_g$, $^1\Sigma_g^+$, $^3\Delta_u$, $A\,^3\Sigma_u^+$, $^1\Sigma_u^-$, and $B\,^3\Sigma_u^-$ states of O_2 have been calculated from spectroscopic data by the Rydberg-Klein-Rees method. Curves for the remaining twelve states of O_2 dissociating-to-ground-state-atoms have been obtained from relations derived from approximate quantum-mechanical calculations, and checked against the meager experimental information available. Two semi-independent calculations have been made, and are in good agreement with each other. The quantum-mechanical relations also lead to an approximate O_2—O_2 interaction, which is consistent with interactions derived from vibrational relaxation times and from high-temperature gas viscosity data.

INTRODUCTION

THIS is the third in a series of papers dealing with the interactions among nitrogen and oxygen atoms and molecules. Such interactions are not only of importance in the calculation of transport properties of air at high temperatures, but a proper knowledge of them may also lead to a better understanding of the chemistry and physics of the upper atmosphere. Previous papers have dealt with the interactions between nitrogen atoms and molecules[1] and between oxygen and nitrogen.[2] The present paper deals with the calculation of the interaction energies between oxygen atoms and molecules.

The most important interactions for the calculation of transport properties are those between the ground state atoms and molecules. When two ground state oxygen atoms (^3P) collide, they can follow any one of eighteen potential energy curves,[3] corresponding to the spectroscopic states $^1\Sigma_g^+(2)$, $^1\Sigma_u^-$, $^1\Pi_g$, $^1\Pi_u$, $^1\Delta_g$, $^3\Sigma_u^+(2)$, $^3\Sigma_g^-$, $^3\Pi_g$, $^3\Pi_u$, $^3\Delta_u$, $^5\Sigma_g^+(2)$, $^5\Sigma_u^-$, $^5\Pi_g$, $^5\Pi_u$, and $^5\Delta_g$. Spectroscopic data are available on the lowest six bound states, $X^3\Sigma_g^-$, $^1\Delta_g$, $^1\Sigma_g^+$, $^1\Sigma_u^-$, $^3\Delta_u$, and $A^3\Sigma_u^+$, as well as on the bound $B^3\Sigma_u^-$ state, which dissociates into a ground state oxygen atom (^3P) and an excited atom (^1D). Accurate potential energy curves for these states have been calculated by the Rydberg-Klein-Rees (RKR) method.[4] For the other states dissociating to ground state atoms the experimental information is meager. Wilkinson and Mulliken[5] suggest that the $^3\Pi_u$ state predissociates the $B\,^3\Sigma_u^-$ state at $v'=12$ on the left-hand side of the minimum of the $B\,^3\Sigma_u^-$ curve. Here v' is the vibrational quantum number of the $B\,^3\Sigma_u^-$ state. They also mention the possibility of a "forbidden" predissociation of the $B\,^3\Sigma_u^-$ state at $v'=3\frac{1}{2}$ by any of the $^5\Sigma_u^-$, $^1\Pi_u$, or $^5\Pi_u$ states. This "forbidden" predissociation would occur on the right-hand side of the minimum of the $B\,^3\Sigma_u^-$ curve.

Simple quantum-mechanical considerations have been used to determine relations among the eighteen different states of O_2 dissociating to ground state atoms. Once the curves for the six bound states are known, these relations enable the "tails" of the other curves to be determined. The curves so calculated agree with the results of Wilkinson and Mulliken on the predis-

* This research was supported in part by the National Aeronautics and Space Administration.

[1] Vanderslice, Mason, and Lippincott, J. Chem. Phys. **30**, 129 (1959).

[2] Vanderslice, Mason, and Maisch, J. Chem. Phys. **31**, 738 (1959).

[3] G. Herzberg, *Spectra of Diatomic Molecules* (D. Van Nostrand Company, Inc., Princeton, New Jersey, 1950), p. 321.

[4] (a) R. Rydberg, Z. Physik **73**, 376 (1931); (b) O. Klein, Z. Physik **76**, 226 (1932); (c) A. L. G. Rees, Proc. Phys. Soc. (London) **59**, 998 (1947); (d) Vanderslice, Mason, Maisch, and Lippincott, J. Mol. Spectroscopy **3**, 17 (1959).

[5] P. G. Wilkinson and R. S. Mulliken, Astrophys. J. **125**, 594 (1957).

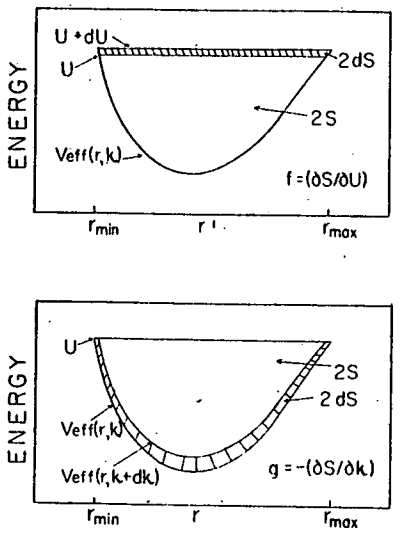

FIG. 1. Graphical interpretation of RKR method.

sociation effects, the only direct experimental checks available. A semi-independent calculation of the "tails," based on the $X^2\Pi$ curve of NO and one O_2 curve, is also in good agreement. These relations have been derived by a modified perfect pairing approximation, previously used[1,2] for N_2 and NO. This modified pairing scheme affords a description in terms of a combination of molecular orbital and valence-bond theory, somewhat along the lines suggested by Linnett.[6] The description further leads to simple relations involving molecules, so that an O_2—O_2 potential can be obtained from results on the O—O interactions. This O_2—O_2 potential is in agreement with other potentials obtained from analysis of high-temperature viscosity data[2] and from analysis of vibrational relaxation time data.[7]

BOUND STATES OF O_2

The potential energy curves for the bound states $X^3\Sigma_g^-$, $^1\Delta_g$, $^1\Sigma_g^+$, $^1\Sigma_u^-$, $^3\Delta_u$, $A\,^3\Sigma_u^+$, and $B\,^3\Sigma_u^-$ were obtained by the RKR method.[4] Although this method has been described in considerable detail in earlier publications,[1,2,4d] it has not been emphasized that the method is quite sensitive to errors in the experimental data in the region near the dissociation limit. To discuss this point, it will suffice here to give a graphical interpretation of the method which follows somewhat along the lines given previously.[4d] The purpose of the method is to obtain values for the classical turning points of the vibrational motion for a given total energy U. The method is formulated in terms of the area $2S$, which is enclosed between the lines of constant energy U and the curve of effective potential energy $V_{eff}(r)$,

$$V_{eff}(r)=V(r)+\kappa/r^2, \qquad (1)$$

where $V(r)$ is the actual potential energy and κ/r^2 is the centrifugal potential term due to rotation (see Fig. 1). The two quantities f and g, defined by

$$f=(\partial S/\partial U)_\kappa \quad \text{and} \quad g=-(\partial S/\partial \kappa)_U, \qquad (2)$$

are then considered. From Fig. 1 it is easy to see that

$$f=\tfrac{1}{2}\int_{r_{min}}^{r_{max}} dr=\tfrac{1}{2}(r_{max}-r_{min}), \qquad (3)$$

$$g=\tfrac{1}{2}\int_{r_{min}}^{r_{max}}(\partial V_{eff}/\partial\kappa)\,dr=\tfrac{1}{2}\int_{r_{min}}^{r_{max}} dr/r^2$$
$$=\tfrac{1}{2}[(1/r_{min})-(1/r_{max})], \qquad (4)$$

where r_{min} and r_{max} are the classical turning points. From these relations it can be seen that a knowledge of $S=S(U,\kappa)$ leads to values of f and g and consequently to values of r_{min} and r_{max}. The RKR method expresses S in terms of the vibrational and rotational constants obtained from analysis of spectroscopic data. Hence once the spectroscopic results are known in a region around U, the function S and consequently r_{min} and r_{max} can be calculated. The method implies that the data are known up to U, since V_{eff} is assumed known up to U in the integration in Eq. (4). This means that the curve has to be built up from the bottom using the spectroscopic data appropriate in each energy region.

It is obvious from the foregoing presentation that f and g are very sensitive to the energy near the dissocia-

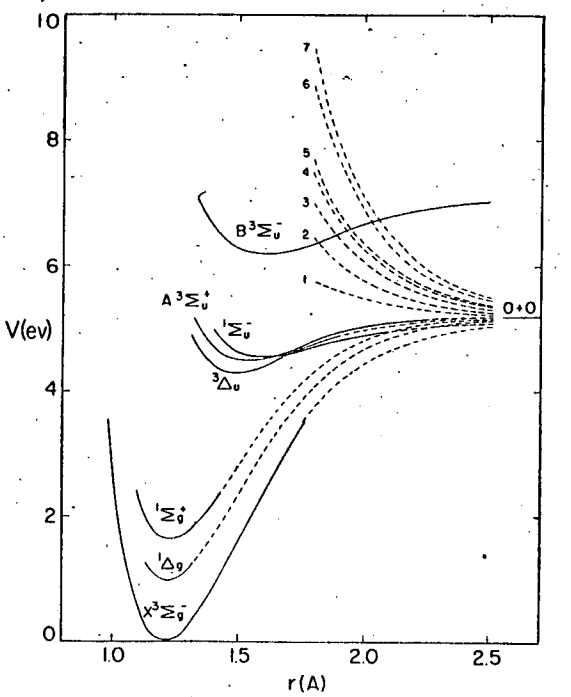

FIG. 2. Summary of O—O interactions. The solid lines have been calculated by the RKR method. The curve numbering is: (1) $^3\Pi_u$ and $^1\Pi_u$; (2) $^5\Pi_g$, $^3\Pi_g$, and $^1\Pi_g$; (3) $^5\Sigma_u^-$ and $^3\Sigma_u^+$; (4) $^1\Sigma_g^+$; (5) $^5\Delta_g$ and $^5\Sigma_g^+$; (6) $^5\Sigma_g^+$; (7) $^5\Pi_u$.

[6] J. W. Linnett, J. Chem. Soc. **1956**, 275.
[7] M. Salkoff and E. Bauer, J. Chem. Phys. **30**, 1614 (1959).

TABLE I. Potential energy of the $X\,^3\Sigma_g^-$ state of O_2.[a]

v	$V(cm^{-1})$	r_{max}(A)	r_{min}(A)	V(ev)
0	787.2	1.262	1.158	0.09761
1	2 344	1.307	1.126	0.2907
2	3 878	1.340	1.106	0.4809
3	5 387	1.370	1.091	0.6680
4	6 873	1.397	1.078	0.8523
5	8 337	1.422	1.067	1.0338
6	9 778	1.445	1.057	1.2125
7	11 196	1.469	1.049	1.3883
8	12 591	1.491	1.041	1.5613
9	13 963	1.513	1.034	1.7314
10	15 313	1.534	1.027	1.8988
11	16 640	1.556	1.022	2.0634
12	17 945	1.577	1.016	2.2252
13	19 227	1.598	1.011	2.3841
14	20 486	1.619	1.006	2.5403
15	21 722	1.641	1.002	2.6935
16	22 934	1.662	0.997	2.8438
17	24 122	1.683	0.993	2.9911
18	25 287	1.704	0.989	3.1356
19	26 429	1.725	0.985	3.2772
20	27 546	1.747	0.982	3.4157
21	28 639	1.768	0.979	3.5512

[a] Experimental data from references 8–12.

tion limit, since small changes in U or κ give large changes in S there. Any errors in the experimental data or inaccuracies in the equations used to fit the data will cause a large error in r. This effect can be seen in the calculated curve for the $B\,^3\Sigma_u^-$ state (see Table VII and Fig. 2), in which the repulsive side of the curve has a positive slope near the dissociation limit. Such a situation does not seem to have occurred before, probably because previous work has not been so close to the dissociation limit.

The results obtained for the bound states by the RKR method are given in Tables I–VII, and the actual curves are shown as the solid lines in Fig. 2. The experimental data were obtained from the following sources: Herzberg,[8a,9] Broida and Gaydon,[8b] Babcock and Herzberg,[10] Lochte-Holtgreven and Dieke,[11] Feast,[12] Herzberg and Herzberg,[13] Hornbeck and Hopfield,[14] Pillow,[15] Brix and Herzberg,[16] Knauss and Ballard,[17] and Herman.[18]

There is some uncertainty in the numbering of the vibrational levels of the $A\,^3\Sigma_u^+$, $^1\Sigma_u^-$, and $^3\Delta_u$ states. Herzberg[9] has assumed that the first measured band in the $^1\Sigma_u^-\leftarrow{}^3\Sigma_g^-$ system is the 1–0 band and that the first diffuse band observed by Herman[18] at 2913 A is the 0–0 band of the $^3\Delta_u\leftarrow{}^3\Sigma_g^-$ system. Broida and Gaydon,[8b] on the basis of their more recent experimental work on the oxygen afterglow, have concluded that Herzberg's vibrational assignments for the $A^3\Sigma_u^+$ state should be increased by one unit. If Herzberg's numbering is used for these states, the $^3\Delta_u$ curve lies below the $A^3\Sigma_u^+$ curve over the entire region covered in this calculation. The $^1\Sigma_u^-$ curve lies below both at large values of r, but crosses the $^3\Delta_u$ curve at $r=1.718$ A and the $A^3\Sigma_u^+$ curve at $r=1.628$ A. This crossing is in disagreement with the conclusions of Moffitt[19] and of Fumi and Parr,[20] who have calculated that the $^1\Sigma_u^-$ curve lies below the $^3\Delta_u$ curve over the whole region. As pointed out by Herzberg, a shift of two units in the numbering of the $^1\Sigma_u^-$ vibrational bands would lower the $^1\Sigma_u^-$ curve below the other two. On the other hand, the theoretical foundations of the electronic structure calculations are not so well established that the results of Moffitt and of Fumi and Parr can be taken as completely reliable. However, since there appears to be some experimental evidence that Herzberg's vibra-

TABLE II. Potential energy of the $^1\Delta_g$ state of O_2[a,b]

v	$V(cm^{-1})$	r_{max} (A)	r_{min} (A)	V (ev)	T_e+V (ev)
0	751.4	1.272	1.166	0.09318	1.0750
1	2235	1.319	1.134	0.2771	1.2589

[a] Experimental data from reference 13.
[b] T_e is the energy difference between the bottom of the potential curve for the state in question and the bottom of the curve for the $X\,^3\Sigma_g^-$ state.

TABLE III. Potential energy of the $^1\Sigma_g^+$ state of O_2.[a]

v	$V(cm^{-1})$	r_{max} (A)	r_{min} (A)	V (ev)	T_e+V (ev)
0	712.9	1.285	1.176	0.08840	1.7245
1	2118	1.334	1.144	0.2626	1.8987
2	3495	1.371	1.123	0.4333	2.0694
3	4843	1.403	1.107	0.6006	2.2367
4	6164	1.432	1.094	0.7643	2.4004

[a] Experimental data from reference 10.

TABLE IV. Potential energy of the $^3\Delta_u$ state of O_2.[a]

v	$V(cm^{-1})$	r_{max} (A)	r_{min} (A)	V (ev)	T_e+V (ev)
0	454.0	1.557	1.420	0.05630	4.3543
1	1323	1.628	1.385	0.1641	4.4621
2	2141	1.685	1.363	0.2655	4.5635
3	2907	1.739	1.347	0.3605	4.6585
4	3621	1.791	1.334	0.4491	4.7471
5	4284	1.844	1.323	0.5312	4.8292
6	4895	1.898	1.312	0.6070	4.9050

[a] Experimental data from references 9 and 18.

[8] (a) G. Herzberg, Can. J. Phys. **30**, 185 (1952); (b) H. P. Broida and A. G. Gaydon, Proc. Roy. Soc. (London) **A222**, 181 (1954).
[9] G. Herzberg, Can. J. Phys. **31**, 657 (1953).
[10] H. D. Babcock and L. Herzberg, Astrophys. J. **108**, 167 (1948).
[11] W. Lochte-Holtgreven and G. H. Dieke, Ann. Physik **3**, 937 (1929).
[12] M. W. Feast, Proc. Phys. Soc. (London) **A63**, 549 (1950).
[13] L. Herzberg and G. Herzberg, Astrophys. J. **105**, 353 (1947).
[14] G. A. Hornbeck and H. S. Hopfield, J. Chem. Phys. **17**, 982 (1949).
[15] M. E. Pillow, Proc. Phys. Soc. (London) **A67**, 847 (1954).
[16] P. Brix and G. Herzberg, Can. J. Phys. **32**, 110 (1954).
[17] H. P. Knauss and S. S. Ballard, Phys. Rev. **48**, 796 (1935).
[18] L. Herman, Ann. Physik **11**, 548 (1939).
[19] W. Moffitt, Proc. Roy. Soc. (London) **A210**, 224 (1951).
[20] F. G. Fumi and R. G. Parr, J. Chem. Phys. **21**, 1864 (1953).

TABLE V. Potential energy of the $A\ ^3\Sigma_u^+$ state of O_2.

v	$V(cm^{-1})$	r_{max} (A)	r_{min} (A)	V (ev)	T_e+V (ev)
(a) Experimental data and vibrational assignments from reference 8a.					
0	383.1	1.608	1.461	0.04751	4.5343
1	1127	1.683	1.421	0.1397	4.6265
2	1838	1.743	1.397	0.2279	4.7147
3	2513	1.798	1.380	0.3116	4.7984
4	3149	1.853	1.365	0.3905	4.8773
5	3742	1.908	1.351	0.4640	4.9508
6	4284	1.971	1.342	0.5313	5.0181
7	4770	2.043	1.334	0.5915	5.0783
8	5188	2.133	1.327	0.6433	5.1301
9	5524	2.257	1.322	0.6849	5.1717
(b) Experimental data from reference 8a and vibrational assignments from reference 8b.					
0	397[a]	1.600	1.454	0.04923	4.4382
1	1172[a]	1.669	1.412	0.1453	4.5343
2	1916	1.724	1.386	0.2375	4.6265
3	2627	1.775	1.367	0.3257	4.7147
4	3302	1.825	1.351	0.4094	4.7984
5	3938	1.877	1.339	0.4883	4.8773
6	4530	1.931	1.328	0.5618	4.9508
7	5073	1.993	1.319	0.6291	5.0181
8	5559	2.064	1.311	0.6893	5.0783
9	5977	2.154	1.305	0.7411	5.1301
10	6313	2.277	1.300	0.7828	5.1717

[a] These values have been obtained by extrapolation.

tional assignments for the $A^3\Sigma_u^+$ state may be incorrect, we have calculated two potential curves for this state, one using Herzberg's assignments,[8a] and one using the assignments of Broida and Gaydon.[8b] These are given in Tables V(a) and (b). In the subsequent discussion, we have used the curve based on Herzberg's assignments. Our conclusions would be unchanged if the other $A\ ^3\Sigma_u^+$ curve were used.

POTENTIAL CURVES AT LARGE DISTANCES FOR BOUND STATES OF O_2

The RKR method gives results only in regions where spectroscopic data are available. It can be seen from Fig. 2 that the solid RKR lines do not extend to large values of r. For many purposes it is necessary to have potential curves at the larger distances.

The $^1\Delta_g$ and $^1\Sigma_g^+$ curves were fitted by Hulburt-Hirschfelder functions[21] at large distances. The Hulburt-Hirschfelder function appears to be about the best empirical potential available, although it does not fit the lowest state ($X\ ^3\Sigma_g^-$) very well. These curves for the $^1\Delta_g$ and $^1\Sigma_g^+$ states are shown as dashed lines in Fig. 2. The RKR curves for these states are not known over a large enough range of r to furnish a stringent test of the fit of the empirical potential curves, but an indirect check can be obtained. According to Mulliken[22] (see also Moffitt[19]), the energy splittings between the three lowest states, $X\ ^3\Sigma_g^-$, $^1\Delta_g$, and $^1\Sigma_g^+$, should be about equal. Actually, the ratio of the splittings is about 1.48 over the known range. If this ratio is assumed constant for all values of r, then a potential at large r can be calculated for the $X\ ^3\Sigma_g^-$ state from the two empirical potential curves for the $^1\Delta_g$ and $^1\Sigma_g^+$ states. This calculated curve, which can be represented by the equation

$$V(r) = -452.4e^{-3.176r}\ \text{ev}, \qquad 1.7\text{A} < r < 2.5\ \text{A}, \quad (5)$$

is also shown dashed in Fig. 2. This dashed line joins on fairly smoothly to the RKR curve for the ground state, thereby giving an indirect check on the other two curves. The constants for the Hulburt-Hirschfelder curves are given in Table VIII.

The RKR curves for the $^1\Sigma_u^-$, $^3\Delta_u$, and $A^3\Sigma_u^+$ states are known over a large enough range of r to test rigorously any empirical potential function. The $^3\Delta_u$ state was best represented at large distances by a Hulburt-Hirschfelder curve, whereas the $^1\Sigma_u^-$ state was fitted satisfactorily with a Morse curve. The constants

TABLE VI. Potential energy of the $^1\Sigma_u^-$ state of O_2.[a]

v	$V(cm^{-1})$	r_{max} (A)	r_{min} (A)	V (ev)	T_e+V (ev)
0	321.0	1.678	1.517	0.03980	4.5880
1	941.2	1.764	1.476	0.1167	4.6649
2	1522	1.833	1.452	0.1887	4.7369
3	2067	1.899	1.435	0.2563	4.8045
4	2574	1.964	1.421	0.3191	4.8673
5	3042	2.030	1.410	0.3772	4.9254
6	3470	2.098	1.400	0.4303	4.9785

[a] Experimental data from reference 9.

TABLE VII. Potential energy of the $B\ ^3\Sigma_u^-$ state of O_2.[a]

v	$V(cm^{-1})$	r_{max} (A)	r_{min} (A)	V (ev)	T_e+V (ev)
0	348.2	1.683	1.531	0.04318	6.2187
1	1036	1.756	1.486	0.1285	6.3040
2	1701	1.813	1.459	0.2110	6.3865
3	2343	1.865	1.438	0.2905	6.4660
4	2960	1.914	1.420	0.3671	6.5426
5	3553	1.962	1.405	0.4405	6.6160
6	4114	2.009	1.392	0.5101	6.6856
7	4648	2.057	1.380	0.5764	6.7519
8	5149	2.112	1.370	0.6384	6.8139
9	5614	2.172	1.362	0.6961	6.8716
10	6043	2.235	1.353	0.7493	6.9248
11	6431	2.302	1.344	0.7975	6.9730
12	6777	2.386	1.342	0.8403	7.0158
13	7077	2.480	1.338	0.8776	7.0531
14	7332	2.588	1.334	0.9092	7.0847
15	7542	2.721	1.335	0.9352	7.1107
16	7711	2.872	1.340	0.9561	7.1316
17	7844	3.055	1.345	0.9726	7.1481
18	7946	3.270	1.354	0.9853	7.1608
19	8021	3.536	1.364	0.9946	7.1701
20	8074	3.900	1.370	1.0012	7.1767

[a] Experimental data from references 16 and 17.

[21] H. M. Hulburt and J. O. Hirschfelder, J. Chem. Phys. 9, 61 (1941).

[22] R. S. Mulliken, Revs. Modern Phys. 4, 1 (1932).

for these curves are also given in Table VIII, and the curves themselves are shown dashed in Fig. 2. The $A\,^3\Sigma_u^+$ state (based on Herzberg's assignment) could not be fitted over its whole range by any of the usual empirical functions, but a Morse function could be adjusted to give an excellent fit from 1.74 to 2.26 A, and extrapolation to 2.5 A should be reliable. The equation for this curve is

$$V(r)=0.7267\{\exp[-10.58(r-1.599)]-2\exp[-5.29(r-1.599)]\}\text{ev},\quad 1.74\text{ A}<r<2.5\text{ A}. \quad (6)$$

RELATIONS AMONG THE STATES OF O_2

A number of approximate but useful relations among the eighteen states of O_2 can be obtained from simple quantum-mechanical considerations. These relations can be used to calculate the long-range "tails" of the curves for the remaining twelve states from the results for the six known bound states discussed in the preceding sections. The results should be fairly reliable since theory is used only to obtain relations among energies and not to calculate directly the energies themselves. Only the p electrons are considered. Similar procedures seemed to work well for N_2[1] and NO,[2] and we might therefore expect it to give good results for O_2 as well.

Since we are interested primarily in the long-range "tails" of the potential energy curves, a correlation among the energies of the various states should presumably be developed by a valence-bond (VB) method, which is generally the best simple method at large internuclear distances,[23] and which gives a description of the molecular states in terms of atomic orbitals (AO's). This involves essentially an electron pairing procedure, which receives its simplest formulation in the perfect pairing approximation,[24]

$$V=\sum_{\substack{\text{orbitals with}\\ \text{paired spins}}}J_{ij}-\tfrac{1}{2}\sum_{\substack{\text{orbitals with}\\ \text{nonpaired spins}}}J_{ij}-\sum_{\substack{\text{orbitals with}\\ \text{parallel spins}}}J_{ij}, \quad (7)$$

where V is the interaction energy and J_{ij} is the exchange integral for two electrons in the atomic orbitals

TABLE VIII. Parameters of empirical functions which give best fit for the bound states of O_2.

$V=D_e[(1-e^{-x})^2+cx^3e^{-2x}(1+bx)-1]$; $x=2\beta(r-r_e)/r_e$

State	D_e(ev)	r_e(A)	2β	c	b
$^1\Delta_g$	4.230	1.2155	3.4203	0.089501	2.6976
$^1\Sigma_g^+$	3.576	1.2268	3.5637	0.098629	2.9187
$^1\Sigma_u^-$	0.6653	1.597	4.8841	0	...
$^3\Delta_u$	0.9154	1.4804	5.4637	0.021247	1.3282

[23] (a) C. A. Coulson, *Valence* (Oxford University Press, New York, 1952), pp. 147–151; (b) Eyring, Walter, and Kimball, *Quantum Chemistry* (John Wiley & Sons, Inc., New York, 1944), pp. 214, 241.

[24] Reference 23a, pp. 166–184.

TABLE IX. Simple MO description of the lower states of N_2 together with their VB energy expressions.

MO's	$X\,^1\Sigma_g^+$	$A\,^3\Sigma_u^+$	$^5\Sigma_g^+$	$^7\Sigma_u^+$
$\sigma_u(2p_{x1}-2p_{x2})$				↑
$\pi_g^-(2p_{z1}-2p_{z2})$		↑	↑	↑
$\pi_g^+(2p_{y1}-2p_{y2})$			↑	↑
$\pi_u^-(2p_{z1}+2p_{z2})$	↑ ↓	↑	↑	↑
$\pi_u^+(2p_{y1}+2p_{y2})$	↑ ↓	↑ ↓	↑	↑
$\sigma_g(2p_{x1}+2p_{x2})$	↑ ↓	↑ ↓	↑ ↓	↑
VB energy expression	$J_{xx}+J_{yy}+J_{zz}$	$J_{xx}+J_{yy}-J_{zz}$	$J_{xx}-J_{yy}-J_{zz}$	$-J_{xx}-J_{yy}-J_{zz}$

i and j. In the foregoing equation terms involving the coulomb integrals have been omitted, since the coulombic interaction between neutral atoms is very small at large internuclear separations. On the other hand, there are many advantages to a molecular orbital (MO) formulation of the problem, since the electronic configurations of molecular states have a very clear and simple description in MO language. This is an important consideration for O_2 with its eighteen states. We therefore try to establish a simple connection between the MO and AO descriptions, such that we can describe the electron configurations in MO language, and from this description write down VB expressions for the interaction energies. Such a connection on a simple level is not trivial, since the MO and the VB or AO descriptions on this level are basically different, inasmuch as the MO description is in terms of *single* electrons and the AO description is in terms of *pairs* of electrons. Of course, in their higher approximations the two descriptions become equivalent,[23] but we are seeking to avoid as much as possible the complications of higher approximations. A further advantage of a simple connection between the MO and the AO descriptions is that it suggests modifications and extensions of the perfect pairing approximation which are necessary for some cases.

Let us first consider a case for which both the VB and the MO descriptions are clear cut, and for which the perfect pairing approximation, Eq. (7), is known to lead to reliable results. The interaction between two ^4S nitrogen atoms, $N(1s)^2(2s)^2(2p_x)(2p_y)(2p_z)$, leads to four possible molecular states, $X\,^1\Sigma_g^+$, $A\,^3\Sigma_u^+$, $^5\Sigma_g^+$, and $^7\Sigma_u^+$. When two N atoms approach each other, the three electrons in the p orbitals of each atom can be paired together in various ways: pairing all three leads to the $X\,^1\Sigma_g^+$ state of N_2; pairing two electrons of one atom with two of the other atom and antipairing the third electrons (spins parallel) leads to the $A^3\Sigma_u^+$ state; and so on until the $^7\Sigma_u^+$ state results from all the p electrons being antipaired. According to Eq. (7) the interaction energies are therefore

$$V(^1\Sigma)=J_{xx}+J_{yy}+J_{zz}=J_{xx}+2J_{yy},$$

$$V(^3\Sigma)=J_{xx}+J_{yy}-J_{zz}=J_{xx},\text{ etc. (see Table IX)}, \quad (8)$$

TABLE X. Simple MO description of the lower states of O_2 together with VB energy expressions.

MO's	$X\,^3\Sigma_g^-$	$^1\Delta_g$	$^1\Sigma_g^+$	$^1\Sigma_u^-$	$^3\Delta_u$	$A\,^3\Sigma_u^+$
$\sigma_u(2p_{x1}-2p_{x2})$						
$\pi_g^-(2p_{z1}-2p_{z2})$	↑		↓	↑ ↓	↑	↑ ↓
$\pi_g^+(2p_{y1}-2p_{y2})$	↑	↑ ↓	↑	↓	↑ ↓	↑
$\pi_u^-(2p_{z1}+2p_{z2})$	↑ ↓	↑ ↓	↑ ↓	↑	↑	↑
$\pi_u^+(2p_{y1}+2p_{y2})$	↑ ↓	↑ ↓	↑ ↓	↑ ↓	↑ ↓	↑ ↓
$\sigma_g(2p_{x1}+2p_{x2})$	↑ ↓	↑ ↓	↑ ↓	↑ ↓	↑ ↓	↑ ↓
VB energy expression	$J_{xx}-J_{yy}$	$J_{xx}-J_{yy}$	$J_{xx}-J_{yy}$	$J_{xx}-3J_{yy}$	$J_{xx}-3J_{yy}$	$J_{xx}-3J_{yy}$

where the x axis lies along the internuclear axis, and by symmetry $J_{xx}\neq J_{yy}=J_{zz}$. In Eq. (8), cross terms such as J_{xy} have been neglected. The reason for doing so is that these terms are smaller than the diagonal terms such as J_{xx}. The exchange term, J, consists of a large number of integrals but, in general, the value of J is roughly proportional to the overlap integral[23b] which by symmetry is zero for the cross terms.

It is clear from Eq. (8) that a knowledge of any two of the states enables one to solve for J_{xx} and J_{yy} and from these the energies of the other two states can be calculated. This has been done for N_2 with excellent results.[1]

It is worth mentioning that a more rigorous scheme would include terms like J_{xy} in Eq. (8). We have not done so since there are not at present sufficient data to evaluate the additional terms which would arise. The inclusion of these additional terms should serve to make the agreement with experiment even better. The results obtained with the present scheme justify this approach—at least until more experimental data become available.

The simple MO description of these four states of N_2 is given in Table IX, together with the VB energy expressions. The MO's, σ_g, π_u^+, π_u^-, π_g^+, π_g^-, and σ_u,† are also shown as approximated by a linear combination of atomic orbitals (LCAO), and it is evident from symmetry that $\pi_u^\pm$ and $\pi_g^\pm$ form two degenerate sets. The relation between the MO and VB descriptions is clear from Table IX: a pair of electrons in a bonding MO leads to a contribution of $+J$ according to the VB perfect pairing approximation, whereas the combination of one electron in a bonding MO plus another electron of the same spin in the corresponding antibonding MO leads to a contribution of $-J$. This latter point has been previously pointed out in some detail by Linnett,[6] who showed that the simple MO wave function for two such electrons, which in Slater determinants is

$$|\,\pi_u^+\alpha \quad \pi_g^+\alpha\,|, \tag{9}$$

is entirely equivalent in the LCAO approximation, except for a normalization factor, to a VB wave function in terms of AO's, which is

$$|\,2p_{y_1}\alpha \quad 2p_{y_2}\alpha\,|. \tag{10}$$

These simple relations serve as a guide for the more complicated case of O_2. From the MO description of the various molecular states which arise from the interaction of ground state atoms, one should be able to write down the VB expressions for the interaction energies. Since the simple VB description yields results which are in general superior to the simple MO results at large internuclear separations, such a procedure should yield valuable results, as it does for N_2.

The foregoing procedure cannot be applied to O_2 without modification and extension. To illustrate why this is so, we consider the six lowest states of O_2, whose simple MO description is given in Table X. In this simple description there are a number of different electron distributions for the $^1\Delta_g$, $^1\Sigma_g^+$, $^1\Sigma_u^-$, $^3\Delta_u$ and $^3\Sigma_u^+$ states which are degenerate with the ones given in the table. The MO wave functions for these states therefore have to be represented by linear combinations of the wave functions associated with the different electron distributions. Allowance for the use of linear combinations will lead to splitting, causing, for example, the $^1\Sigma_g^+$ state to have a different energy than either the $^1\Delta_g$ or the $^3\Sigma_g^-$ state. This splitting might be looked on as a second-order effect, and it is not included in the present approximation. Such splitting may be fairly large, but we expect that its effects would not be greater in any case than the energy difference between the $^3\Sigma_g^-$ and $^1\Sigma_g^+$ states. Neglecting this effect, then, we see from Table X that there are three electron configurations which did not occur in N_2. These configurations are

$$\begin{array}{lccc} \pi_g^\pm & \uparrow & \uparrow\downarrow & \uparrow\downarrow \\ \pi_u^\pm & \uparrow\downarrow & \uparrow\downarrow & \uparrow \\ & \text{(A)} & \text{(B)} & \text{(C)} \end{array} \tag{11}$$

The method of treating these electrons from a VB viewpoint is suggested by the work of Linnett.[6] Consider the arrangement (A). As mentioned previously, Linnett has shown that two electrons with α spin, of

† These MO's are also often denoted as $\sigma 2p_z$, $\pi 2p_y$, $\pi 2p_z$, $\pi^* 2p_y$, $\pi^* 2p_z$, and $\sigma^* 2p_z$, respectively.

which one is in a bonding π_u MO and the other is in an antibonding π_g MO, can be considered equivalent to one electron with α spin in each separate AO. If a third electron with β spin is now added to the bonding π_u MO, Linnett has shown that the situation can still be described as the two electrons with α spin occupying AO's and the one electron with β spin occupying the π_u MO. According to Eq. (7) the pair of electrons in the AO's contribute an amount $-J_{vv}$ to the interaction energy. The electron in the bonding π_u MO forms a one-electron bond, and the strength of such a bond is usually about one-half the strength of the corresponding two-electron bond.[23] Thus the total contribution to the interaction energy from the "three-electron bond" of configuration (A) is about $-\frac{1}{2}J_{vv}$.‡ The "three-electron bond" energy has been discussed in the earlier paper[2] on NO, where it was shown that the results obtained on this basis are quite reasonable, and consistent with the meager spectroscopic data and with the large difference in dissociation energy between NO and NO^+.

Consider now the arrangement (B). It is easy to show by the rules of determinants that, within the LCAO approximation, the simple MO wave function

$$|\,\pi_u{}^+\alpha \quad \pi_u{}^+\beta \quad \pi_g{}^+\alpha \quad \pi_g{}^+\beta\,| \qquad (12)$$

is entirely equivalent, except for a normalizing factor, to the simple VB bond wave function

$$|\,2p_{v_1}\alpha \quad 2p_{v_1}\beta \quad 2p_{v_2}\alpha \quad 2p_{v_2}\beta\,|. \qquad (13)$$

According to (13), we can think of the two electrons of α spin on the different atoms contributing an energy of $-J_{vv}$, and similarly for the electrons of β spin, for a total contribution of $-2J_{vv}$. Alternatively, (13) can be interpreted as two electrons on each atom having their spins internally paired, and hence randomly oriented (nonpaired) with respect to the spins of the two electrons on the other atom. According to Eq. (7), this interpretation leads to an energy contribution of $4(-\frac{1}{2}J_{vv}) = -2J_{vv}$, as before.

Finally, the arrangement (C) can also be treated by the Linnett procedure, and is obviously equivalent to one electron with α spin in each AO plus one electron with β spin in the antibonding π_g MO. The two electrons in the AO's contribute $-J_{vv}$ to the energy, but the third electron in the antibonding MO contributes $-\frac{3}{2}J_{vv}$. This has to be so if the configuration

$$\begin{matrix} \pi_g{}^{\pm} & \uparrow \\ \pi_u{}^{\pm} & \uparrow \end{matrix} \qquad (14)$$

is to give a net contribution of $-J_{vv}$ as dictated by the perfect pairing relation. The one electron in the π_u MO has been assumed to contribute $+\frac{1}{2}J_{vv}$, so that the electron in the π_g MO must contribute to $-\frac{3}{2}J_{vv}$ to make the sum be $-J_{vv}$. Thus the total contribution from configuration (C) is $-\frac{5}{2}J_{vv}$. This can also be seen in an even simpler way. Configuration (C) is equivalent to (B) with one electron removed from a bonding MO and hence the energy of (C) is $-2J_{vv}-(+\frac{1}{2}J_{vv}) = -\frac{5}{2}J_{vv}$.

With these rules, then, we can immediately write down the energy expressions for the six lowest states of O_2. These are given in Table X, where we have again set $J_{vv}=J_{zz}$. To the approximation of neglecting splitting, it is seen that the six states break up into two sets of three states each. This is in approximate agreement with experiment, as can be seen in Fig. 2.

The foregoing discussion suggests that the whole method can be formally treated completely on the basis of single electrons, and all reference to electron pairs eliminated. If we assign a contribution to the interaction energy of $+\frac{1}{2}J$ for a single electron in a bonding MO, and $-\frac{3}{2}J$ for a single electron in an antibonding MO, the correct VB energy expression can be obtained simply by adding up the contributions of all the electrons. It seems somewhat paradoxical that an energy expression for electron pairing can be written down in terms of single electron energies, but reference to the preceding discussion and to Tables IX and X shows the validity of the procedure. This result greatly simplifies the problem of writing down energy expressions for large numbers of complicated

‡ Since the arguments used to obtain this value are at best heuristic, the referees have suggested that a more detailed comment should be made. Consider the wave function $|\,a\alpha\, b\alpha\, (a+b)\beta\cdots m\alpha\, n\beta\,|$, where the functions a, b, c, etc., are assumed normalized on the respective atoms. This wave function corresponds to the "three-electron bond" involving the AO's a and b, which are associated with the like atoms A and B. The terms in the interaction energy arising from this three-electron bond are

$$V_3 \approx -(ab\ ab)_H + (ab)_H,$$

where we have as usual neglected the multiple exchange and coulomb integrals, and where

$$(ab\ ab)_H = \int (a_1a_2b_3c_4\cdots)H(b_1a_2a_3c_4\cdots)d\tau,$$

$$(ab)_H = \int (a_1a_2b_3c_4\cdots)H(a_1b_2b_3c_4\cdots)d\tau.$$

We now want to relate this result to the energies of the one-electron bond and of the repulsive two-electron bond with parallel spins. The wave function for the repulsive two-electron bond between a and b is $|\,a\alpha\, b\alpha\cdots n\beta\,|$, and leads to a contribution to the interaction energy of

$$V_2 \approx -(ab\ ab)_H,$$

which we have set equal to $-J_{vv}$. Similarly, the wave function for the one-electron bond between a and b is $|\,(a+b)\alpha\cdots n\beta\,|$, and leads to a contribution to the interaction energy of

$$V_1 \approx (ab)_H,$$

which we have assumed to have half the strength of a normal attractive two-electron bond, or $\frac{1}{2}J_{vv}$. The interaction energy for the three-electron bond is therefore

$$V_3 = V_2 + V_1 = -\tfrac{1}{2}J_{vv}.$$

Thus, the value we have used in this paper is consistent with our assumption regarding the strength of the one-electron bond. In a similar manner it can be shown that the configuration (C) of (11) leads to an interaction energy of $-\frac{3}{2}J_{vv}$.

TABLE XI. Electronic configurations and energy expressions for the upper states of O_2.

State	Electronic configuration (MO)	Energy (VB)	Energy in terms of $^1\Delta_g$ and $^3\Delta_u$
$^3\Pi_u$ $^1\Pi_u$	$\sigma_g^2(\pi_u^+)^2(\pi_u^-)^2\pi_g^+(\alpha)\sigma_u(\alpha)$ $\sigma_g^2(\pi_u^+)^2(\pi_u^-)^2\pi_g^+(\alpha)\sigma_u(\beta)$	$-\frac{1}{2}(J_{xx}-J_{yy})$	$-\frac{1}{2}V(^1\Delta_g)$
$^5\Pi_g$ $^3\Pi_g$ $^1\Pi_g$	$\sigma_g^2(\pi_u^+)^2\pi_u^-(\alpha)\pi_g^+(\alpha)\pi_g^-(\alpha)\sigma_u(\alpha)$ $\sigma_g^2(\pi_u^+)^2\pi_u^-(\alpha)\pi_g^+(\alpha)\pi_g^-(\alpha)\sigma_u(\beta)$ $\sigma_g^2(\pi_u^+)^2\pi_u^-(\alpha)\pi_g^+(\beta)\pi_g^-(\alpha)\sigma_u(\beta)$	$-\frac{1}{2}(J_{xx}+3J_{yy})$	$-\frac{3}{2}V(^1\Delta_g)+V(^3\Delta_u)$
$^5\Sigma_u^-$ $^3\Sigma_u^+$	$\sigma_g(\alpha)(\pi_u^+)^2(\pi_u^-)^2\pi_g^+(\alpha)\pi_g^-(\alpha)\sigma_u(\alpha)$ $\sigma_g(\alpha)(\pi_u^+)^2(\pi_u^-)^2\pi_g^+(\alpha)\pi_g^-(\beta)\sigma_u(\alpha)$	$-(J_{xx}+J_{yy})$	$-2V(^1\Delta_g)+V(^3\Delta_u)$
$^1\Sigma_g^+$	$\sigma_g^2(\pi_u^+)^2(\pi_u^-)^2\sigma_u^2$	$-2(J_{xx}-J_{yy})$	$-2V(^1\Delta_g)$
$^5\Delta_g$ $^5\Sigma_g^+$	$\sigma_g(\alpha)(\pi_u^+)^2\pi_u^-(\alpha)(\pi_g^+)^2\pi_g^-(\alpha)\sigma_u(\alpha)$ $\sigma_g(\alpha)(\pi_u^+)^2\pi_u^-(\alpha)\pi_g^+(\alpha)(\pi_g^-)^2\sigma_u(\alpha)$	$-(J_{xx}+3J_{yy})$	$-3V(^1\Delta_g)+2V(^3\Delta_u)$
$^5\Sigma_g^+$	$\sigma_g^2\pi_u^+(\alpha)\pi_u^-(\alpha)\pi_g^+(\alpha)\pi_g^-(\alpha)\sigma_u^2$	$-2(J_{xx}+J_{yy})$	$-4V(^1\Delta_g)+2V(^3\Delta_u)$
$^5\Pi_g$	$\sigma_g(\alpha)(\pi_u^+)^2\pi_u^-(\alpha)\pi_g^+(\alpha)\pi_g^-(\alpha)\sigma_u^2$	$-\frac{1}{2}(5J_{xx}+3J_{yy})$	$-\frac{3}{2}V(^1\Delta_g)+2V(^3\Delta_u)$

molecular electronic states, and we believe it combines the best features of both the MO and VB theories in their simplest forms.

The simple MO description of the other twelve states of O_2 is given in Table XI, together with the energy expressions obtained by the above scheme. As in Table X, we have given only one configuration for each state, although several configurations are possible for many of the states. As mentioned previously, this will lead to splitting so that the states shown as degenerate in Table XI will actually be split, although we do not believe such splitting should be greater than that observed for the three lowest states of O_2.

It is now possible to write expressions for the energies of all the states in Table XI in terms of the energies of any two other states. We choose the $^1\Delta_g$ and $^3\Delta_u$ states since these are the intermediate ones in the two groups of known states. The resulting expressions are given in the final column of Table XI. The energies of these different states in the range from 1.8 to 2.5 A can be represented as follows:

$$^3\Pi_u, {}^1\Pi_u: V(r)=339\,e^{-3.570r}\text{ ev}, \quad (15)$$

$$^5\Pi_g, {}^3\Pi_g, {}^1\Pi_g: V(r)=717\,e^{-3.565r}\text{ ev}, \quad (16)$$

$$^5\Sigma_g^+: V(r)=2114\,e^{-3.567r}\text{ ev}, \quad (17)$$

$$^1\Sigma_g^+: V(r)=1358\,e^{-3.570r}\text{ ev}, \quad (18)$$

$$^5\Pi_u: V(r)=2455\,e^{-3.567r}\text{ ev}, \quad (19)$$

$$^5\Sigma_u^-, {}^3\Sigma_u^+: V(r)=1057\,e^{-3.567r}\text{ ev}, \quad (20)$$

$$^5\Delta_g, {}^5\Sigma_g^+: V(r)=1433\,e^{-3.565r}\text{ ev}. \quad (21)$$

These curves are shown in Fig. 2 as dashed lines. They can, of course, be extrapolated to larger distances than 2.5 A, but at the expense of increased uncertainty in their values.

The only experimental information on any of these curves comes from an analysis of predissociation effects in the $B\,^3\Sigma_u^-$ curve. Wilkinson and Mulliken[5] find that there is certainly predissociation at the $v'=12$ level of the $B\,^3\Sigma_u^-$ curve, and it is probable that predissociation takes place in the whole range from $v'=4$ to $v'=12$. According to the correlation rules and the selection rules for predissociation,[25] only the $^3\Pi_u$ state can predissociate the $B\,^3\Sigma_u^-$ state strongly. Wilkinson and Mulliken suggest that the $^3\Pi_u$ curve predissociates the $B\,^3\Sigma_u^-$ curve by crossing it to the left of the minimum at $v'=12$. They further suggest that the $^3\Pi_u$ curve comes close to the $B\,^3\Sigma_u^-$ curve most of the way up the left-hand side of the curve, and that this could explain the probable predissociation in all levels from $v'=4$ to $v'=12$. Our calculated curve for the $^3\Pi_u$ state rises a little too rapidly to pass entirely on the left-hand side of the $B\,^3\Sigma_u^-$ curve from the minimum to $v'=12$. Extrapolation of our curve inward indicates that it cuts the $B\,^3\Sigma_u^-$ not only at about $v'=12$, but also right at the minimum. Wilkinson and Mulliken rule out the possibility of a double crossing of the $B\,^3\Sigma_u^-$ curve by the $^3\Pi_u$ curve, once at the minimum and once at $v'=12$, because of the absence of any observed predissociation effects at the $v'=0$ and $v'=1$ levels. It is therefore probable that our $^3\Pi_u$ curve is slightly too high around the region of the minimum of the $B\,^3\Sigma_u^-$ curve, but this is easily explained by the approximations we have made.§ Allowance for the effect of splitting would lower our $^3\Pi_u$ curve, and inclusion of the cou-

[25] Reference 3, Chap. VII, Sec. 2.

§ *Note added in proof.*—After this article had been submitted for publication, Dr. Wilkinson called our attention to Dr. P. K. Carroll's work on predissociation in the Schumann-Runge bands [Astrophys. J. **129**, 794 (1959)]. Carroll reports a predissociation at $v'=4$ which apparently is stronger than the predissociation at $v'=12$. He suggests that this may be caused by the $^3\Pi_u$ curve crossing on the right-hand side of the $^3\Sigma_u^-$ curve at $v'=4$. If this is so, then it is difficult to explain the other predissociations ranging from $v'=4$ up to $v'=12$, especially the fact that the probability for predissociation appears to have two maxima, one at $v'=4$ and another at $v'=11$ with a minimum at $v'=9$. Carroll has also found abnormally wide widths for the rotational lines in the 2–0 and 1–0 bands of the Schumann-Runge bands. He feels that this is due to a blending of fine structure components. Our explanation would be that the $^3\Pi_u$ curve crosses at the bottom of the $^3\Sigma_u^-$ curve, as is suggested by our calculations, and then rises along the left-hand branch as Wilkinson and Mulliken suggest.

lombic and overlap integrals dropped from Eq. (7) would cause it to rise fairly sharply at small internuclear separations. If we use the crossing point at $v'=12$ ($V=1.801$ ev, $r=1.342$ A) together with our values for the $^3\Pi_u$ curve at large distances, the equation

$$V(r)=7.61\exp(-0.8224\,r^2)\text{ ev},\qquad 1.34\text{ A}<r<2.5\text{ A}\quad(22)$$

gives an excellent fit. Equation (22) is not entirely correct, however, since it still crosses the $B\,^3\Sigma_u^-$ curve at the minimum, and it is entirely probable that it should pass beneath the minimum. Further evidence for this is the apparent observation by Wilkinson and Mulliken of a weak continuum under the Schumann-Runge bands which may be attributable to the transition $^3\Pi_u \leftarrow {}^3\Sigma_g^-$.

Wilkinson and Mulliken also rule out the crossing of the $B\,^3\Sigma_u^-$ curve by the $^3\Pi_u$ curve at about $v'=3$ on the right-hand side of the minimum, a suggestion made by Flory[26] to explain certain photochemical effects. They suggest that the photochemical results can be explained by a "forbidden" predissociation near $v'=3\frac{1}{2}$ by any of the $^5\Sigma_u^-$, $^1\Pi_u$, or $^5\Pi_u$ curves. Our results indicate that the $^5\Sigma_u^-$ curve crosses the $B^3\Sigma_u^-$ curve right at $v'=3\frac{1}{2}$.

Our results, therefore, are at least not inconsistent with the meager experimental information that is available on the repulsive states which dissociate to ground state atoms. It can further be shown that they are consistent with the previously calculated[2] NO energies, on the assumption that the exchange integrals J are about the same for NO and O_2. Since the energy for the $^2\Pi$ ground state of NO is $V(^2\Pi, \text{NO})=J_{xx}+\frac{1}{2}J_{yy}$, and that for the $^3\Delta_u$ state of O_2 is $V(^3\Delta_u, O_2)=J_{xx}-3J_{yy}$, we can calculate J_{xx} and J_{yy} as a function of distance from the known energies and use the values to calculate the energy of the $^1\Delta_g$ state of O_2. The energies of the $^1\Delta_g$ and $^3\Delta_u$ states in turn determine the energies of all the other O_2 states, as has been shown in Table XI. The $^1\Delta_g$ energies calculated in this way agree with the values of Table VIII quite well. The deviation is 0.010 ev at $r=1.8$ A, rises to 0.041 ev at $r=2.1$ A, and falls to 0.018 ev at $r=2.6$ A. These deviations propagate directly to the other O_2 states as shown by the last column of Table XI. The agreement is certainly within the uncertainty caused by our neglect of splitting.

O_2—O_2 INTERACTIONS

The modified perfect pairing scheme describes interactions between molecules as just the sums of the interactions between the constituent atoms, so that we can calculate approximately the long-range O_2—O_2 interaction from the results of the preceding sections.

[26] P. J. Flory, J. Chem. Phys. **4**, 23 (1936).

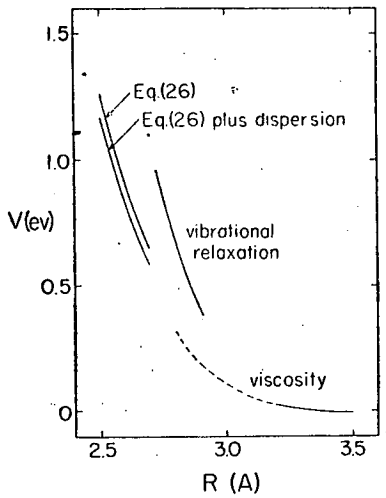

FIG. 3. Average O_2—O_2 interaction as obtained by different methods.

Similar procedures worked well for the N_2—N_2 and N_2—O_2 interactions.[1,2] Consider the interaction of an oxygen atom, $O(2p_x)(2p_y)^2(2p_z)$, with another oxygen atom, $O(2p_x)(2p_y)(2p_z)^2$, each of which is bound to another oxygen to form two oxygen molecules. The interaction of these two configurations will lead to the lowest energy. The electron spins on these two atoms are uncorrelated (nonpaired), and by the perfect pairing relation the net interaction energy between the two atoms is

$$V(\text{O}\cdots\text{O})=-\tfrac{1}{2}J_{xx}-\tfrac{1}{2}(2J_{yy})-\tfrac{1}{2}(2J_{zz})=-\tfrac{1}{2}J_{xx}-2J_{yy},\|\quad(23)$$

or from Table X,

$$V(\text{O}\cdots\text{O})=-\tfrac{1}{4}[7V(^1\Delta_g)-5V(^3\Delta_u)],\quad(24)$$

which can be represented by the expression

$$V(\text{O}\cdots\text{O})=812\,e^{-3.565r}\text{ ev},\quad 1.8\text{ A}<r<2.5\text{ A}.\quad(25)$$

The O_2—O_2 interactions are obtained by adding up all the four pertinent O···O interactions, each of which is given by Eq. (25) with the value of r appropriate for the atom-atom distance. The dependence of the O_2—O_2 interaction on orientation is thus given implicitly by the dependence of the atom-atom distances on the molecular orientations.

In many cases it is useful to have the total O_2—O_2 interaction energy averaged over all orientations. The

|| The referee has pointed out that the interaction energy calculated in this way does not take into account the fact that the values of J_{xx} and J_{yy} depend on the relative orientation of the two O_2 molecules, as well as the fact that at certain orientations the cross terms such as J_{xy} become large. Consideration of extremes of orientations shows that these effects introduce a maximum variation with orientation of about 40% into Eqs. (23)–(25). Neglect of this variation is thus consistent with the other approximations involved, such as neglect of multiple exchange integrals [E. A. Mason and J. O. Hirschfelder, J. Chem. Phys. **26**, 756 (1957)], inasmuch as the J's are really treated as disposable parameters to be determined from experiment. Furthermore, the final averaging over all molecular orientations to obtain Eq. (26) also tends to compensate the error.

method of averaging has already been given in connection with the N_2—N_2 interaction,[1] and leads to the result

$$\langle V(R)\rangle = 5580\, e^{-3.365r} \text{ ev}, \quad 1.93\text{ A} < r < 2.70\text{ A}, \qquad (26)$$

where R is the distance between the centers of mass of the molecules. This result can be compared with similar potential energies obtained from analysis of measurements of high-temperature gas viscosity[2] and of vibrational relaxation times.[7] The viscosity result has been given as an exp-six potential, and the vibrational relaxation result as a Morse potential. The comparison is shown in Fig. 3. Since Eq. (26) is the result of essentially only a first-order perturbation calculation, it is of interest to add on the second-order perturbation energy, the London dispersion energy, which is given approximately as

$$\langle V(\text{dis})\rangle = -\tfrac{3}{4}(\bar{\alpha}^2 I/R^6) = -(24.0/R^6) \text{ ev}, \quad R \text{ in A}, \qquad (27)$$

where $\bar{\alpha}$ is the average polarizability of an O_2 molecule and I its ionization potential. The sum of Eqs. (26) and (27) is also shown in Fig. 3. The agreement among the potentials, calculated in three completely independent ways, is excellent. The fact that the potential from vibrational relaxation measurements seems high is to be expected from the approximations made in the theory of vibrational relaxation. This theory is in effect a one-dimensional treatment involving the end-to-end molecular configuration.[27] Since this configuration leads to the largest interaction energy of any configuration, the difference shown in Fig. 3 is not unexpected.

SUMMARY

Potential energy curves for the interactions between two ground state O atoms have been calculated from spectroscopic data and from approximate quantum-mechanical relations. The results obtained from spectroscopic data (RKR method) are given in Tables I–VI for the $X\,^3\Sigma_g^-$, $^1\Delta_g$, $^1\Sigma_g^+$, $^3\Delta_u$, $A\,^3\Sigma_u^+$, and $^1\Sigma_u^-$ states of O_2. The long-range "tails" of the $^1\Delta_g$, $^1\Sigma_g^+$, and $^3\Delta_u$ curves were fitted with Hulburt-Hirschfelder functions, whereas the $^1\Sigma_u^-$ curve was best fitted with a Morse function. The constants for these empirical functions are given in Table VIII. The $A\,^3\Sigma_u^+$ curve was found to be best fitted at large r by Eq. (6), and the $X\,^3\Sigma_g^-$ curve at large r was represented by Eq. (5). Relations among the eighteen states of O_2 dissociating to ground state atoms have been obtained by a modified perfect pairing approximation. This is based on a description of electronic configurations in terms of a combination of AO's and MO's which leads to simple rules for writing down a VB energy expression, given a simple MO description of an electronic state. These relations yield results for the repulsive states of O_2 which have been represented by Eqs. (15) through (21). The repulsive states have been checked against predissociation effects observed in the $B\,^3\Sigma_u^-$ state, and are in agreement with the observations. The curve for the $B\,^3\Sigma_u^-$ state, the upper state of the Schumann-Runge bands, has been calculated by the RKR method with the results shown in Table VII. A partial check has also been made by calculating the O_2 curves in terms of the known curves for the $X\,^2\Pi$ state of NO and the $^3\Delta_u$ state of O_2, with satisfactory agreement.

An O_2—O_2 potential has been generated from the O—O potentials in a manner similar to that used for the N_2—N_2 and N_2—O_2 potentials obtained previously.[1,2] The results are consistent with other potentials obtained from different experimental sources.

It is difficult to assess the absolute accuracy of all the results obtained. However, they are all internally consistent and in agreement with the limited available experimental data.

ACKNOWLEDGMENTS

The authors are extremely grateful to Louis T. Ho, who not only performed a large number of calculations for them, but also checked much of their own work. They are also grateful to Ernest Madsen for checking some of the calculations, and to Dr. Ernest Bauer for communicating the results of his vibrational relaxation calculations before their publication.

[27] (a) E. Bauer, J. Chem. Phys. **23**, 1087 (1955); (b) M. Salkoff and E. Bauer, *ibid.* **29**, 26 (1958).